Calcium-Dependent Stabilization of the Central Sequence Between Met^{76} and Ser^{81} in Vertebrate Calmodulin

Zhihai Qin and Thomas C. Squier*
Biochemistry and Biophysics Section, Department of Molecular Biosciences, University of Kansas, Lawrence, Kansas 66045 USA

ABSTRACT Spin-label electron paramagnetic resonance (EPR) provides optimal resolution of dynamic and conformational heterogeneity on the nanosecond time-scale and was used to assess the structure of the sequence between Met^{76} and Ser^{81} in vertebrate calmodulin (CaM). Previous fluorescence resonance energy transfer and anisotropy measurements indicate that the opposing domains of CaM are structurally coupled and the interconnecting central sequence adopts conformationally distinct structures in the apo-form and following calcium activation. In contrast, NMR data suggest that the opposing domains of CaM undergo independent rotational dynamics and that the sequence between Met^{76} and Ser^{81} in the central sequence functions as a flexible linker that connects two structurally independent domains. However, these latter measurements also resolve weak internuclear interactions that suggest the formation of transient helical structures that are stable on the nanosecond time-scale within the sequence between Met^{76} and Asp^{80} in apo-CaM (H. Kuboniwa, N. Tjandra, S. Grzekiek, H. Ren, C. B. Klee, and A. Bax, 1995, *Nat. Struct. Biol.* 2:768–776). This reported conformational heterogeneity was resolved using site-directed mutagenesis and spin-label EPR, which detects two component spectra for 1-oxyl-2,2,5,5-tetramethylpyrroline-3-methyl)-methanethiosulfonate spin labels (MTSSL) bound to CaM mutants T79C and S81C that include a motionally restricted component. In comparison to MTSSL bound within stable helical regions, the fractional contribution of the immobilized component at these positions is enhanced upon the addition of small amounts of the helicogenic solvent trifluoroethanol (TFE). These results suggest that the immobilized component reflects the formation of stable secondary structures. Similar spectral changes are observed upon calcium activation, suggesting a calcium-dependent stabilization of the secondary structure. No corresponding changes are observed in either the solvent accessibility to molecular oxygen or the maximal hyperfine splitting. In contrast, more complex spectral changes in the line-shape and maximal hyperfine splitting are observed for spin labels bound to sites that undergo tertiary contact interactions. These results suggest that spin labels at solvent-exposed positions within the central sequence are primarily sensitive to backbone fluctuations and that either TFE or calcium binding stabilizes the secondary structure of the sequence between Met^{76} and Ser^{81} and modulates the structural coupling between the opposing domains of CaM.

INTRODUCTION

Calmodulin (CaM) is a ubiquitous eukaryotic calcium-binding protein that plays a critical role in intracellular signal transduction pathways (Crivici and Ikura, 1995; Tjandra et al., 1999). The crystal structure of calcium-saturated CaM indicates the presence of two globular domains joined by a solvent-exposed central helix located between Phe^{65} and Phe^{92} (Babu et al., 1985, 1988; Chattopdhyaya et al., 1992) (Fig. 1). Calcium activation of CaM, a prerequisite step for regulation of target proteins, involves a reorientation of the four α-helical bundles within each of the two globular domains with the concomitant exposure of hydrophobic sites that bind target proteins (La Porte et al., 1980; Kuboniwa et al., 1995; Urbauer et al., 1995; Zhang et al., 1995). Many of the structural details of this conformational transition have been documented. However, the presence of structural coupling between the opposing domains of CaM, in which one domain modifies the conformation of the other, and its functional role remains controversial.

Numerous biochemical studies indicate the presence of structural coupling between the opposing globular domains in CaM that may play an important role in modulating the kinetics of target protein activation (Yao et al., 1994; Pedigo and Shea, 1995a,b; Mukherjea et al., 1996; Shea et al., 1996; Sorensen and Shea, 1996; Sun et al., 1999; Jaren et al., 2000). For example, the proteolytic susceptibility or fluorescence intensity of sites in the amino-terminal domain responds to calcium occupancy to sites in the carboxyl-terminal domain (Yao et al., 1994; Pedigo and Shea, 1995a; Shea et al., 1996, 2000; Sorensen and Shea, 1998). Similarly, the modification of sites within the carboxyl-terminal domain (oxidation of either Met^{144} or Met^{145} or the site-directed substitution of Tyr^{138} with Phe^{138}) results in an enhanced rotational mobility of the amino-terminal domain (Gao et al., 1998; Yin et al., 2000a; Sun et al., 2001). There is, however, no consensus on the mechanisms underlying the observed structural linkages between the opposing domains, largely because multidimensional NMR measurements suggest that there are neither direct contact interactions between the opposing domains nor conformational coupling through the interdomain central sequence (Ikura et al., 1991; Barbato et al., 1992; Kuboniwa et al., 1995; Zhang et al., 1995). However, these latter NMR measurements selectively detect ordered structures that exhibit internuclear interactions and cannot resolve conformational

Received for publication 10 January 2001 and in final form 30 July 2001.
Address reprint requests to Dr. Thomas C. Squier, Biochemistry and Biophysics Section, Department of Molecular Biosciences, 5055 Haworth Hall, University of Kansas, Lawrence, KS 66045-2106. Tel.: 785-864-4008; Fax: 785-864-5321; E-mail: tsquier@ukans.edu.

0006-3495/01/11/2908/11 $2.00

FIGURE 1 Mutation sites for site-directed spin labeling with respect to the backbone fold of CaM. Five mutation sites are shown involving F68C, L69C, T79C, S81C, and L105C. Coordinates are 3cln.pdb (Babu et al., 1988), and the illustration was made using the program Molscript (Kraulis, 1991).

heterogeneity on the nanosecond time-scale associated with the intramolecular reorientation of the opposing domains of CaM that is relevant to target protein binding.

Therefore, we have used site-directed spin-label electron paramagnetic resonance (EPR), which is sensitive to the nanosecond time-scale, to assess the dynamic structure of the sequence between Met^{76} and Ser^{81}. Five separate CaM mutants were created, permitting the incorporation of methanethiosulfonate spin-labels (MTSSL) covalently bound to individual cysteines engineered at defined positions within the primary sequence of CaM (Fig. 1). After spin-labeling, these sites permit a comparison of the dynamic structures of the sequence between Met^{76} and Ser^{81}, which have been suggested to be conformationally disordered compared with sites either in more stable regions of the central sequence or in globular domains expected to be sensitive to tertiary contact interactions (Finn et al., 1995; Mchaourab et al., 1996). Thus, individual cysteines were inserted at 1) T79C and S81C within the sequence between Met^{76} and Ser^{81}, 2) at F68C and L69C near the amino terminus of the central helix, and 3) at L105C in a helical site within the carboxyl-terminal globular domain.

We report that spin labels bound to either T79C or S81C, within the conformationally disordered sequence between Met^{76} and Ser^{81}, exhibit a spectral component with motional properties analogous to positions within stable helical regions within the central sequence (i.e., L69C) and that calcium activation stabilizes the motionally restricted conformation resulting in a more conformationally restricted and rigid interdomain sequence. This result is consistent with previous fluorescence measurements that demonstrated conformational changes involving the central sequence between Phe^{65} and Phe^{92}, which are important in the mechanism of calcium activation and target protein binding (Sun et al., 1999), and provides strong evidence that the opposing domains of CaM are structurally coupled through the interdomain sequence that includes the region between Met^{76} and Ser^{81}.

MATERIALS AND METHODS

Materials

1-Oxyl-2,2,5,5-tetramethylpyrroline-3-methyl-methanethiosulfonate spin label (MTSSL) was purchased from Reanal Fine Chemicals (Budapest, Hungary). WP PEI (weak anion exchanger) packing for the HPLC column was from J. T. Baker (Phillipsburg, NJ), and the weak-anion exchange column used to purify CaM was packed in-house. A Micro BCA protein reagent kit was obtained from Pierce (Rockford, IL). HEPES was obtained from Research Organics, Inc (Cleveland, Ohio). All other reagent chemicals were of highest purity available commercially. Erythrocyte ghost plasma membranes were purified from porcine blood, essentially as previously described (Niggli et al., 1979).

Expression and purification of CaM mutants

The coding region for chicken CaM (accession number MCCH (PIR database) or P02593 (SWISS-PROT data base)) was excised from the plasmid pCaMPL provided by Professor Samuel George (Duke University) and subcloned into the mutagenesis and expression vector pALTER-Ex1 (Promega, Madison, WI) using restriction enzymes *Nco*I and *Xba*I. The recombinant plasmid pEx1-CaM was transformed into *Escherichia coli* strain JM109(DE3) for overexpression, as previously described (Studier and Moffatt, 1986; Sun et al., 1999). The sequence of chicken CaM is identical to all other expressed vertebrate CaM, including human, mouse, rat, rabbit, bovine, duck, frog, and salmon (Putkey et al., 1983; Wylie and Vanaman, 1988; Fischer et al., 1988; Kawasaki and Kretsinger, 1995; Friedberg, 1996). Furthermore, the measured mass of the expressed chicken CaM obtained using electrospray ionization mass spectrometry (ESI-MS) is 16,707 ± 3 Da, which is in good agreement with the theoretical mass of 16,706.4 for the following sequence: $ADQLTEEQIA^{10}$ $EFKEAFSLFD^{20}$ $KDGDGTITTK^{30}$ $ELGTVMRSLG^{40}$ $QNPTEAELQD^{50}$ $MINEVDADGN^{60}$ $GTIDFPEFLT^{70}$ $MMARKMKDTD^{80}$ $SEEEIREAFR^{90}$ $VFDKDGNGYI^{100}$ $SAAELRHVMT^{110}$ $LGEKLTDEE^{120}$ $VDEMI-READI^{130}$ $DGDGQVNYEE^{140}$ $FVQMMTAK^{148}$. This sequence contains no endogenous cysteines, permitting us to specifically introduce single cysteines for site-directed spin labeling. In all cases site-directed mutagenesis was carried out as described in the technical manual for the Altered Sites II in vitro mutagenesis system (Promega). Oligonucleotide primers containing the desired mutation were synthesized by Macromolecular Resources (Colorado State University, Ft. Collins, Co.). Correct mutations were ensured by automated DNA sequencing performed in the Biochemical Research Service Laboratory (University of Kansas, Lawrence, KS). Following overexpression, CaM was purified as previously described using phenyl Sepharose-CL-4B (Pharmacia, Piscataway, NJ) and Bakerbond WAX-HPLC (J. T. Baker, Phillipsburg, NJ) (Strasburg et al., 1988; Hühmer et al., 1996). The CaM concentration was determined using the Micro BCA assay (Pierce, Rockford, IL), using salt-free bovine brain CaM as a

standard. The concentration of the CaM standard was determined using the published molar extinction coefficient (ϵ_{277} = 3029 M^{-1} cm^{-1}) for the calcium-saturated enzyme (Strasburg et al., 1988). The purity of the expressed proteins was greater than 99% as indicated by SDS-polyacrylamide gel electrophoresis and ESI-MS. Purified CaM was dialyzed against distilled water and following lyophilization was stored at −70°C.

Covalent modification of CaM with MTSSL spin label

CaM (0.1 mM) was derivatized with a 10-fold molar excess of MTSSL in 25 mM HEPES (pH 7.5) and 1 mM EDTA at 25°C for ~3 h, essentially as previously described (Berliner et al., 1982). The spin-labeled CaM was separated from unbound spin label using weak anion-exchange high-performance liquid chromatography (HPLC), essentially as previously described (Hühmer et al., 1996). Spin-labeled CaM was lyophilized to the desired volume and then dialyzed separately against 25 mM HEPES (pH 7.5), 0.1 M KCl, 1 mM $MgCl_2$, and either 100 μM EGTA or 100 μM $CaCl_2$ to prepare apo- or calcium-saturated CaM. The functional ability of the spin-labeled CaM mutants to activate the plasma membrane Ca-ATPase was assayed as previously described (Lanzetta et al., 1979; Yao et al., 1996).

Spectroscopic measurements

Circular dichroism (CD) spectra of CaM were measured at 25°C with a Jasco J-500C spectrometer using a thermojacketed CD spectral cell with a path-length of 1.0 cm. EPR spectra of 0.1 mM CaM were recorded in 50-μl disposable micropipettes (Rochester Scientific Co., Rochester, NY) in a Bruker ESP 300E X-band spectrometer (Billerica, MA) using a TM102 cavity fitted with a quartz dewar. Unless otherwise specified, spectra were acquired using an incident microwave field (H_1) of 0.1 Gauss, a modulation frequency (H_m) of 100 KHz, and a modulation amplitude (H_m) of 2.0 Gauss. In all cases temperature was controlled to within 0.5°C using a Eurotherm B-VT 2000. Continuous-wave power saturation measurements of spin-labeled CaM were carried out essentially as previously described (Altenbach et al., 1989a; Mchaourab et al., 1996), where the power at which the signal amplitude is half that if no saturation occurred ($P_{1/2}$) was measured in the presence of oxygen saturated air $P_{1/2}$(air) and nitrogen $P_{1/2}(N_2)$. The change in $P_{1/2}$ due to the presence of oxygen ($\Delta P_{1/2}$) is proportional to the collision frequency, where $\Delta P_{1/2} = P_{1/2}(\text{air}) - P_{1/2}(N_2)$ (Altenbach et al., 1989b). Additional terms that correct for spectrometer performance and differences in spin-lattice relaxation times permit a comparison between the solvent accessibilities of different spin-labeled CaM mutants, where the accessibility parameter (Π) is defined as:

$$\Pi = \frac{\Delta P_{1/2} \times \Gamma(\text{DPPH})}{P_{1/2}(\text{DPPH}) \times \Gamma_o}, \qquad (1)$$

where $P_{1/2}$(DPPH) is the $P_{1/2}$ for a DPPH crystal, Γ(DPPH) is the peak-to-peak line-width of the DPPH resonance, and Γ_o is the corresponding line-width of the nitroxide central resonance (Altenbach et al., 1996).

RESULTS

Retention of function following site-specific spin labeling of CaM

Site-directed spin labeling was used to investigate the possible role of the sequence between Met^{76} and Ser^{81} in mediating the structural coupling between the opposing domains of CaM. Five separate CaM mutants were created involving 1) conservative substitutions within the sequence between Met^{76} and Ser^{81} (i.e., T79C or S81C), 2) near the amino terminus of a relatively stable helical structure within the solvent-exposed central sequence between Phe^{65} and Phe^{92} (i.e., F68C, L69C), or 3) within a helical element within the carboxyl-terminal domain in a region expected to undergo significant tertiary contact interactions (i.e., L105C) (Fig. 1). Mutations involving charged amino acids were avoided, as these have previously been shown to stabilize the structure of the central sequence (Sun et al., 1999). In all cases the introduction of individual cysteines and the covalent attachment of MTSSL to these sites results in minimal perturbation of the secondary structure of CaM, because the α-helical content is virtually identical to that of wild-type CaM (Fig. 2; Table 1). Likewise, the CaM dependence of the activation of the plasma membrane Ca-ATPase and the maximal ATPase activity are virtually identical for all five spin-labeled CaM mutants compared with wild-type CaM (Table 1). Thus, the mutation and spin-label modifications do not affect the structure or function of CaM, indicating that spin-label EPR measurements of the rotational dynamics at these positions reflect the native structure of CaM.

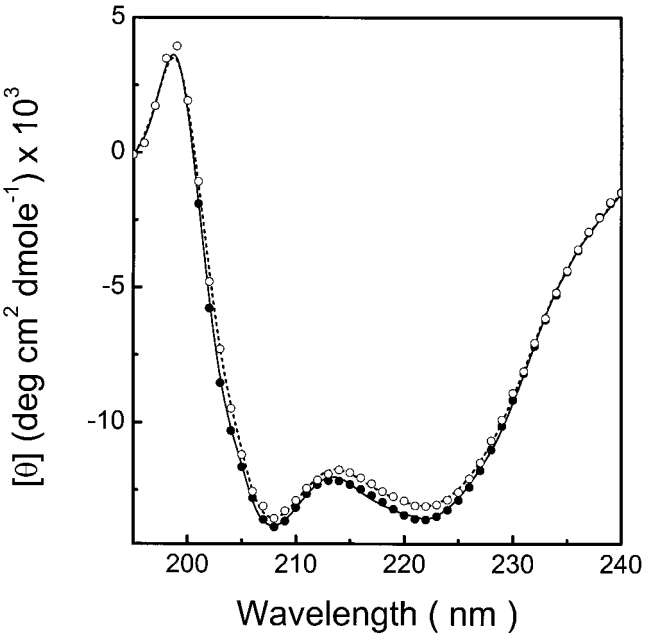

FIGURE 2 Site-directed mutation and spin-labeling does not alter the secondary structure of CaM. Far-UV circular dichroism spectra of wild-type CaM (●) and representative spin-labeled mutant CaM CaMF68C (○) are shown with associated theoretical fits obtained using the program Contin (Venyaminov and Yang, 1996). Experimental conditions involved 6 μM CaM in 10 mM Tris-HCl (pH 7.5), 0.1 M $KClO_4$, 1.0 mM $Mg(ClO_4)_2$, and 0.1 mM $Ca(ClO_4)_2$

Resolution of conformational heterogeneity within the central sequence

In the crystal structure of CaM (1cll.pdb), L69, T79, and S81 do not undergo significant tertiary contact interactions

TABLE 1 Properties of calmodulin mutants

CaM species	ATPase activity (μmol P_i mg^{-1} h^{-1})	α-Helical content	Maximal hyperfine splitting (Gauss)		Line-width (Γ_o) (Gauss)		O_2 accessibility (Π)	
			apo-CaM	$(Ca^{2+})_4$-CaM	apo-CaM	$(Ca^{2+})_4$-CaM	apo-CaM	$(Ca^{2+})_4$-CaM
Wild type	1.5 ± 0.2	57 ± 1%						
F68C	1.3 ± 0.2	57 ± 2%	61 ± 1	55 ± 1	2.1 ± 0.1	3.0 ± 0.1	0.14 ± 0.02	0.11 ± 0.01
L69C	1.3 ± 0.1	56 ± 2%	63 ± 1	62 ± 1	2.8 ± 0.1	2.8 ± 0.1	0.23 ± 0.02	0.23 ± 0.03
T79C	1.4 ± 0.2	58 ± 2%	61 ± 1	61 ± 1	2.9 ± 0.1	3.3 ± 0.1	0.17 ± 0.01	0.16 ± 0.01
S81C	1.5 ± 0.2	59 ± 2%	59 ± 1	59 ± 1	2.4 ± 0.1	2.6 ± 0.1	0.14 ± 0.01	0.15 ± 0.01
L105C	1.2 ± 0.1	59 ± 2%	60 ± 1	51 ± 3	2.2 ± 0.1	2.7 ± 0.1	0.16 ± 0.01	0.11 ± 0.01

Wild-type and CaM mutants were expressed and purified from *E. coli*, as described in Materials and Methods. CaM-dependent rates of ATP hydrolysis for the plasma membrane Ca-ATPase in erythrocyte ghosts was measured in the presence of saturating CaM concentrations, as previously described in detail (Yao et al., 1996). Estimates of α-helical content were obtained from fits to CD spectra using the program Contin (Venyaminov and Yang, 1996). Maximal hyperfine splitting was measured at 4°C by fitting the spectral extrema to a Gaussian line-shape. Line-width of center peak was measured at 25°C. Oxygen accessibility (Π) was measured at 25°C using Eq. 1 in Materials and Methods.

with other structural elements and have calculated surface accessibilities of 49, 63, and 52 $Å^2$. In contrast, tertiary interactions reduce the solvent accessibilities of Phe^{68} and Leu^{105}, which are 7 and 8 $Å^2$, respectively. Therefore, it is of interest to contrast the rotational dynamics of MTSSL bound to the solvent-exposed sites in the CaM mutants L69C, T79C, and S81C, which are expected to be sensitive to differences in backbone dynamics. Two component spectra are observed for MTSSL bound to these sites over a wide temperature range, and representative spectra are shown at 4°C and 25°C (Fig. 3). At both 4°C and 25°C the fractional contribution of the mobile component in the spectra of MTSSL increases in the following order: L69C < T79C < S81C. This result is consistent with previous NMR measurements, which indicated Leu^{69} to be part of a stable helix, whereas Thr^{79} and Ser^{81} are within a sequence that is conformationally disordered and exhibits minimal internuclear interactions on the NMR time-scale (Ikura et al., 1991; Barbato et al., 1992; Kuboniwa et al., 1995; Finn et al., 1995).

The line-shapes of the spin-label EPR spectra at 25°C are diagnostic of solvent-exposed spin labels, consistent with the solvent-exposed location of these amino acids within the crystal structure of CaM (Babu et al., 1988; Chattopdhyaya et al., 1992; Mchaourab et al., 1996). Addition of 30% sucrose has essentially no effect on the spectral line-shape (data not shown), indicating that the spin-label EPR spectra are insensitive to the rotational motion of the entire CaM molecule and reflect the backbone dynamics of the protein. Decreasing the temperature reduces the rate of motion without significantly affecting the average secondary and tertiary structure of CaM, permitting the molecular anisotropy to be resolved on the spin-label EPR time-scale (Tsalkova and Privalov, 1985; Verheyden et al., 1994; Mchaourab et al., 1996; Sun et al., 2001). Thus, at 4°C the components are clearly separated in the low-field region and indicate the presence of a mobile (β) and motionally restricted (α) component. The maximal hyperfine splitting of the motionally restricted component is similar at all three positions (i.e., L69C, T79C, and S81C) (Table 1), indicating that the rotational dynamics and environment are similar. However, the fractional contribution of the mobile population of spin labels (β) is larger for T79C and S81C (within the disordered sequence between Met^{76} and Ser^{81}) relative to L69C within the solvent-exposed central helix that are expected to be within stable helices. Calcium binding enhances the spectral contribution of the motionally restricted component at T79C and S81C, without affecting the maximal hyperfine splitting (Fig. 3 *A*). Because polarity differences arising from tertiary contact interactions are expected to alter the maximal hyperfine splitting (Mchaourab et al., 1996), these results suggest that the observed spectral changes are sensitive to differences in the secondary structure and backbone dynamics at these solvent-exposed positions.

A consideration of the spin-label EPR spectra at 4°C indicates that irrespective of the spin label position the maximal hyperfine splitting of the EPR spectra is substantially less than 68 G, which is characteristic of a rigid-limit spectrum, suggesting the presence of rotational motion on the nanosecond time-scale (Columbus et al., 2001). This result is consistent with previous fluorescence anisotropy measurements that found fluorophores bound to L69C to undergo restricted rotational motion, with rotational correlation times of 1.9 ± 0.3 ns and 13 ± 1 ns corresponding to segmental motion and the overall rotational motion of CaM (Sun et al., 1999). Likewise, MTSSL bound to sites within helical elements of T4 lysozyme undergoes restricted rotational motion, with a rotational correlation time of ~2 ns, whose amplitude of motion is affected by the placement of the spin label within the sequence (Columbus et al., 2001). Hubbell and co-workers emphasized that the sensitivity of MTSSL to changes in backbone dynamics is directly related to interactions between the disulfide linkage of the spin label and main-chain atoms within the protein, which restrict the amplitude of motion for the nitroxide moiety (Langren et al., 2001). Thus, within solvent-exposed helices it is expected that MTSSL will selectively monitor backbone fluctuations on the nanosecond time-scale that alters the amplitude of probe motion.

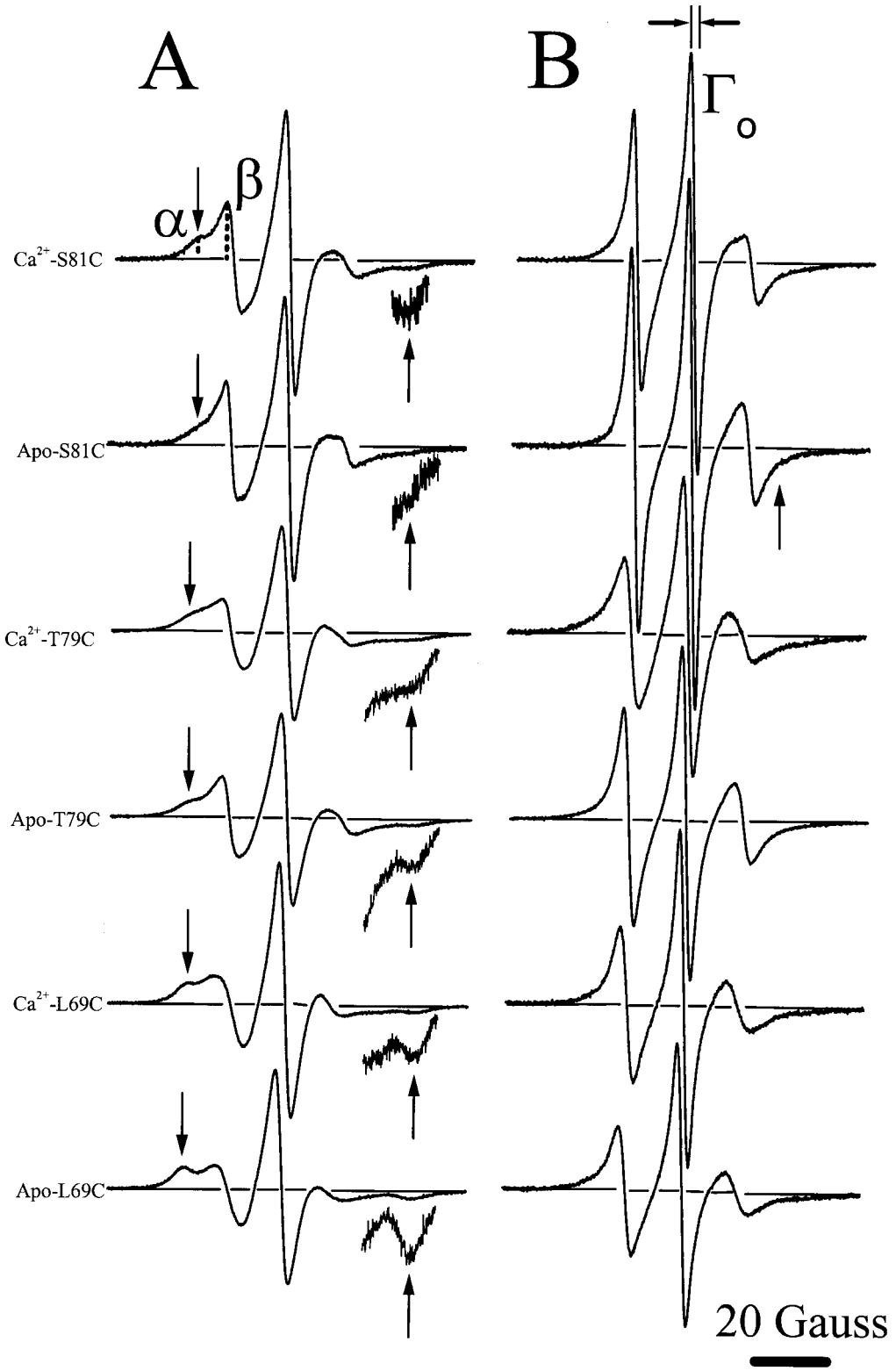

FIGURE 3 Conformational heterogeneity within the central helix is modulated by calcium activation. CaM mutants L69C, T79C, and S81C were individually spin-labeled and spectra were taken at 4°C (*A*) and 25°C (*B*) in the apo- and calcium-activated forms. Corresponding spectral features involving the immobilized (α) and mobile (β) spectral components, the maximal hyperfine splitting (*arrows*), and central field line-width (Γ_o) are indicated in *A* and *B*. For clarity, the high-field extremes are shown expanded 10-fold. Experimental conditions involved 100 μM CaM in 25 mM HEPES (pH 7.5), 0.1 M KCl, 1.0 mM $MgCl_2$, and either 0.1 mM $CaCl_2$ or 0.1 mM EGTA.

The suggestion that MTSSL selectively monitors backbone fluctuations is consistent with the observation that "at the majority of helix surface sites investigated so far, the sequence-specific mobility differences are apparently not determined by differences in interaction with the nearest neighbors in the same helix" (Columbus et al., 2001). Thus, the two component spectra of MTSSL bound to L69C, T79C, and S81C probably represent multiple-protein conformational states. This interpretation is consistent with previous NMR measurements that demonstrated the presence of conformational heterogeneity within the sequence between Met^{76} and Ser^{81}, which "adopts a helical conformation for about one-third of the time" that is relatively stable on the nanosecond time-scale and may transiently adopt a 3_{10} conformation (Kuboniwa et al., 1995). Nevertheless, it is significant that two distinct orientations were observed for the disulfide group of MTSSL in the crystal structure of the spin-labeled R119C mutant of T4 lysozyme, suggesting that conformational heterogeneity can arise because of probe heterogeneity (Langren et al., 2000). One conformation corresponds to a relatively mobile component and is suggested to correspond to a conformer in which the disulfide linkage of MTSSL undergoes a S···N non-hydrogen-bonding interaction with Gln at the $i + 4$ position. This is the only example of the four positions studied in which an interaction with a neighboring side chain resulted in the stabilization of two distinct rotamers of the MTSSL spin label. However, a similar non-hydrogen-bonding interaction between a neighboring Gln in the primary sequence and the disulfide in MTSSL is observed for the K65C mutant, suggesting that interactions between MTSSL and neighboring Gln side chains may result in the appearance of spectral heterogeneity (Langren et al., 2000). The absence of comparable side chains in the vicinity of the sequence between Met^{76} and Ser^{81} makes it unlikely that corresponding interactions occur between MTSSL and proximal side chains in CaM. Nevertheless, it remains possible that the two component spectra of MTSSL bound to sites within CaM could result from probe heterogeneity that is unrelated to protein structural heterogeneity.

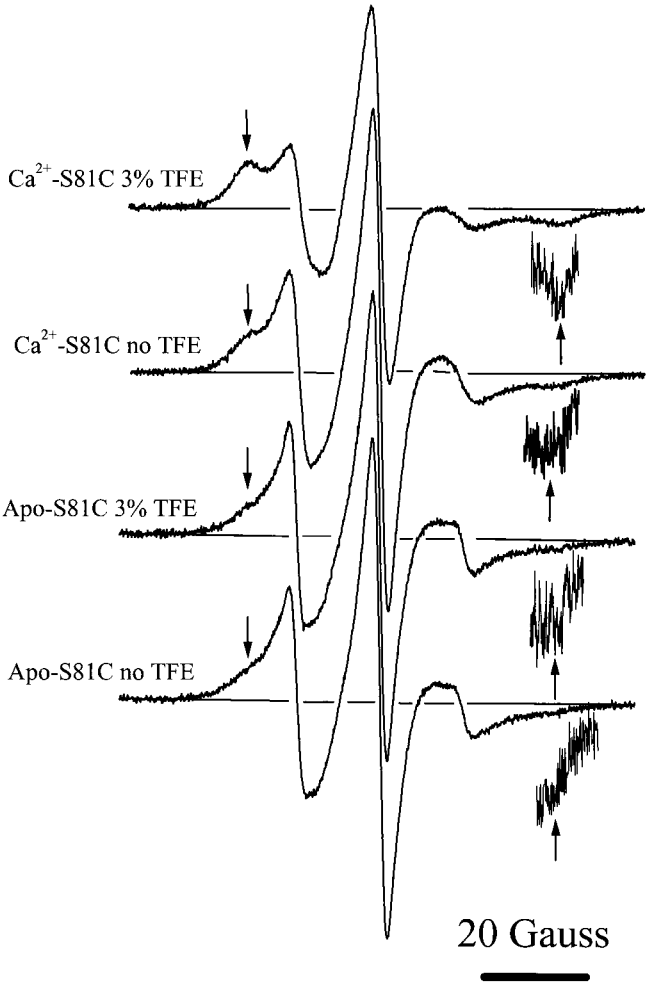

FIGURE 4 Calcium and TFE stabilize the central helix. Spectra for the apo- and calcium-activated forms of the spin-labeled CaM mutant S81C are shown in the absence and presence of 3% (v/v) TFE. High-field extremes are shown expanded 10-fold. Experimental conditions involved 100 μM CaM in 25 mM HEPES (pH 7.5), 0.1 M KCl, 1.0 mM $MgCl_2$, and either 0.1 mM $CaCl_2$ or 0.1 mM EGTA. Temperature was 4°C.

Trifluoroethanol stabilizes the motionally restricted component

To investigate the possible relationship between the two motional populations observed in the spin-label EPR spectra and protein secondary structural elements, we have investigated the dynamic structure of the S81C spin-labeled CaM mutant (which exhibits a substantial mobile component) in the presence of trifluoroethanol (TFE), which has previously been shown to stabilize α-helical structures in a range of proteins including CaM (Bayley and Martin, 1992; Evans, 1995; Luo and Baldwin, 1997). In fact, the use of nonaqueous solvents that stabilize α-helical structures has been suggested to result in the stabilization of the helix between Met^{76} and Ser^{81} in the crystal structure of CaM (Babu et al., 1988; Bayley and Martin, 1992).

We find that the addition of as little as 3% (v/v) TFE stabilizes the motionally restricted conformation for both apo- and calcium-activated CaM (Fig. 4). No alteration in the maximal hyperfine splitting occurs, indicating that at these concentrations TFE selectively stabilizes the immobilized component without significantly affecting the polar environment in the vicinity of the spin label. In contrast, substantially larger amounts of TFE are required to induce line-shape changes in the EPR spectra of MTSSL at F68C and L105C (Fig. 5), which are within more stable helical regions of CaM (Kuboniwa et al., 1995; Zhang et al., 1995; Finn et al., 1995). These results demonstrate a differential sensitivity of MTSSL bound within the sequence between Met^{76} and Ser^{81}relative to more stable secondary structural

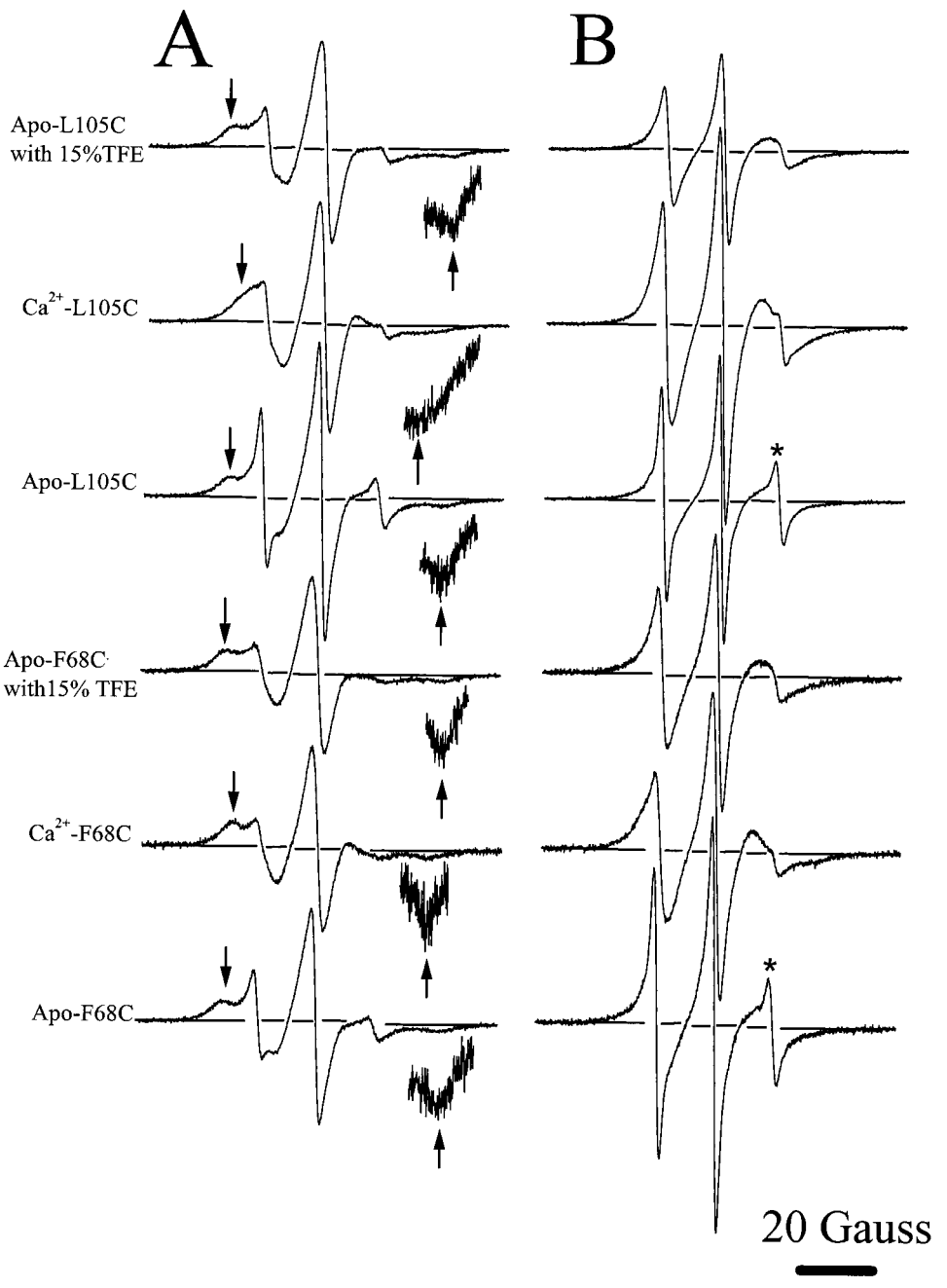

FIGURE 5 Calcium activation alters tertiary contact interactions within individual domains. CaM mutants F68C and L105C were individually spin-labeled and spectra were taken at 4°C (*A*) and 25°C (*B*) in the apo- and calcium-activated forms and in the presence of 15% (v/v) TFE. Corresponding spectral features involving the immobilized (α) and mobile (β) spectral components, the maximal hyperfine splitting (*arrows*), and central field line-width (Γ_o) are as defined in Fig. 3. High-field extremes are shown expanded 10-fold. Experimental conditions involved 100 μM CaM in 25 mM HEPES (pH 7.5), 0.1 M KCl, 1.0 mM $MgCl_2$, and either 0.1 mM $CaCl_2$ or 0.1 mM EGTA in the absence or presence of 15% (v/v) TFE.

elements within either the amino- or carboxyl-terminal domains of CaM. Because denaturation of CaM following the addition of guanidine hydrochloride enhances the fractional contribution of the mobile component (β) (data not shown), these results further suggest that there is a dynamic equilibrium within this sequence between a mobile conformation and a motionally restricted conformation that are in slow exchange on the spin-label EPR time-scale. Thus, in the context of earlier NMR results that suggest the sequence between Met^{76} and Ser^{81} adopts a helical conformation approximately one-third of the time (Kuboniwa et al., 1995), these results suggest that the immobilized component reflects the helical conformation within this sequence. Because calcium binding stabilizes the immobilized component, these results further suggest that calcium binding mediates a direct coupling between the opposing domains of CaM through the stabilization of the helical content between Met^{76} and Ser^{81}.

Tertiary contact interactions modify maximal hyperfine splitting and solvent accessibility

In comparison with MTTSL bound to L69C, T79C, and S81C, calcium-dependent changes in the maximal hyperfine

splitting are evident for spin-labeled CaM mutants F68C and L105C (Fig. 5). These results are consistent with the presence of tertiary contact interactions between side chains at these positions within the crystal structure of CaM (Babu et al., 1988; Chattopdhyaya et al., 1992) and suggest that L69C represents the first residue within the central sequence that does not undergo significant tertiary contact interactions with side chains in other secondary structural elements. Before calcium binding, the rotational mobility of the mobile spectral component (β) for spin labels covalently bound to positions 68 and 105 is larger relative to those bound at solvent-exposed positions (i.e., L69C, T79C, and S81C), as is evident from their larger spectral intensity and the smaller spectral line-widths associated with the center field resonance (Γ_o) (Figs. 3 and 5; Table 1). The enhanced rotational dynamics of the mobile component at these sites may reflect the ability of MTSSL to access a variety of conformations that minimize steric interactions with other side chains at buried sites (Langren et al., 2000). Alternatively, the enhanced mobility may reflect main-chain segmental movements that reflect the partial unwinding of the α-helices at positions 68 and 105, which are, respectively, located at the amino terminus of helices within the crystal structure of CaM (Babu et al., 1988; Chattopdhyaya et al., 1992). Consistent with this latter hypothesis, the addition of 15% (v/v) TFE enhances the spectral contribution of the immobilized fraction of spin labels (Fig. 5 *A*). Likewise, the CaM sequence near Leu^{105} has previously been demonstrated to form a noncompact and disordered state with a highly susceptible proteolytic cleavage site at Arg^{106} (Newton et al., 1984; Tsalkova and Privalov, 1985; Kuboniwa et al., 1995; Shea et al., 1996). These latter results suggest that to be accessible to the active site of the protease that the backbone fold exhibits some nonhelical behavior.

DISCUSSION

Structure and function of the central sequence

The structural coupling between the opposing domains of CaM was originally evident in the crystal structure of CaM. This structure demonstrates two homologous globular domains that include amino acid residues that are part of a central sequence, which exists as an extended α-helix between Phe^{65} and Phe^{92} (Babu et al., 1985, 1988; Chattopdhyaya et al., 1992) (Fig. 1). However, the existence of a stable central sequence in the cell remains controversial, because inclusion of nonaqueous solvents during crystallization stabilizes the helical content within the central sequence (Ikura et al., 1991; Barbato et al., 1992; Bayley and Martin, 1992). Furthermore, under cellular conditions, techniques that monitor the solution structure have demonstrated static disorder within the central sequence that results in a distribution of conformations that modifies the spatial arrangement of the opposing domains (Heidorn and Trewhella, 1988; Yao et al., 1994; Tjandra et al., 1995; Kuboniwa et al., 1995). It is, therefore, often argued that the central sequence functions as a flexible tether, whose major function is to maintain the spatial proximity between the opposing domains necessary for target protein binding (Persechini and Kretsinger, 1988; Kretsinger, 1992; Tjandra et al., 1999). Despite the flexibility of the central sequence, at physiologically relevant ionic strength and pH the central sequence assumes conformationally distinct structures in the apo-form and following calcium activation (Small and Anderson, 1988; Yao et al., 1994; Sorensen and Shea, 1996; Wriggers et al., 1998; Sun et al., 1999). In this respect, mutations that affect the structure of the central sequence diminish the binding affinity between CaM and target proteins (Craig et al., 1987; Kataoka et al., 1991; Sacks et al., 1996; Yin et al., 2000b; Sun et al., 2001). These latter results suggest that stabilization of the central sequence may function to minimize nonspecific interactions between the opposing domains of CaM involved in binding to target proteins. The calcium-dependent stabilization of the structure of the central sequence between Met^{76} and Ser^{81} observed in the present study, therefore, have important implications with respect to the mechanism of target protein binding by CaM.

Conformational heterogeneity within the central sequence of CaM

In this study we have used site-directed spin labeling coupled with the introduction of unique cysteines to resolve calcium-induced conformational changes within the sequence between Met^{76} and Ser^{81} in vertebrate CaM. Two component spectra were observed for MTSSL spin labels covalently bound at positions T79C and S81C in the solvent-exposed interdomain central sequence of CaM using spin-label EPR spectroscopy (Fig. 3), which is indicative of heterogeneity involving the backbone dynamics of CaM. Calcium activation, which was reproduced by the addition of as little as 3% (v/v) TFE, enhances the spectral contribution associated with the immobilized component at positions T79C and S81C (Figs. 3 and 4). Because TFE has previously been demonstrated to stabilize the α-helical content of CaM and other proteins (Bayley and Martin, 1992; Evans, 1995; Luo and Baldwin, 1997), the immobilized component probably reflects a population of helical secondary structures (within the interdomain sequence between Met^{76} and Ser^{81}) that are stabilized by calcium binding. In contrast, much larger amounts of TFE are required to induce line-shape changes at positions F68C or L105C, consistent with their greater conformational stability (Fig. 5). These results are consistent with previous suggestions that the sequence between Met^{76} and Ser^{81} is "delicately balanced between helical and non-helical conformations" (Kuboniwa et al., 1995) and adopts multiple conformations in which a relatively long-lived helical conformation is assumed for

about one-third of the time in apo-CaM (Kataoka et al., 1991; Kretsinger, 1992; Kuboniwa et al., 1995; Wriggers et al., 1998).

The underlying reasons for conformational heterogeneity within the central sequence have been suggested to involve both 1) the transient disruption of specific hydrogen bonds, which can induce the unwinding of helical elements, and 2) a reorientation of the opposing globular domains that favors target protein binding (Wriggers et al., 1998). The presence of multiple conformations within the central sequence that undergo slow exchange on the nanosecond time-scale is, furthermore, consistent with previous suggestions that conformational rearrangements between the opposing domains of CaM are slow relative to the time-scale of overall protein rotational motion, which has been measured using both fluorescence anisotropy and NMR spectroscopy to be between 9 and 12 ns at 20°C (Small and Anderson, 1988; Török et al., 1992; Barbato et al., 1992; Yao et al., 1994; Sun et al., 1999). Thus, in the context of these prior observations, the current results demonstrating that a significant fraction of the interdomain central sequence is conformationally restricted provides strong evidence that the calcium-dependent structural linkage between the opposing domains of CaM involves alterations in the structure of the interdomain central sequence between Met^{76} and Ser^{81}.

Significance of central sequence to high-affinity CaM binding

Previous measurements have demonstrated that initial binding between CaM and target proteins normally involves the high-affinity association of the carboxyl-terminal domain of CaM followed by association of the amino-terminal domain. Association of the amino-terminal domain is aided by the reduced volume available for its diffusion following the initial association of the carboxyl-terminal domain (Persechini and Kretsinger, 1988; Persechini et al., 1993, 1994; Sun and Squier, 2000). Disruption of the α-helical structure within the central sequence is required for both domains of CaM to bind to target proteins and is part of a conformational switch that occurs following the initial association of the carboxyl-terminal domain to initiate the collapse of CaM around CaM-binding sequence in target proteins (Ikura et al., 1992; Meador et al., 1992, 1993; Yao and Squier, 1996; Sun et al., 2001). Therefore, the marginal stability of the sequence between Met^{76} and Ser^{81} in solution may be part of a conformational switch that facilitates target protein activation (Barbato et al., 1992; Wriggers et al., 1998; Sun et al., 1999). In this respect, the extended conformation of CaM (whose structure has been stabilized under crystallization conditions) has been suggested to facilitate high-affinity binding to target proteins by minimizing competitive interdomain contact interactions (Yin et al., 2000b; Sun et al., 2001). Our present results suggest that calcium-induced increases in the fraction of helix around Thr^{79} and Ser^{81} facilitate high-affinity target protein binding by minimizing interdomain interactions. Consistent with this suggestion, a reduced binding affinity to target proteins is apparent in CaM variants with sequence differences within calcium-binding site four that results in the loss of high-affinity calcium binding and structural interactions between the opposing domains (Lee and Klevit, 2000; Yin et al., 2000b). Likewise, the binding affinity between CaM and target proteins is diminished following the structural uncoupling between the opposing domains by oxidative modification of selected methionines near the carboxy terminus or the elimination of the hydrogen bond between Trp^{138} and Glu^{82} (Gao et al., 1998; Yin et al., 2000a; Sun et al., 2001). All of these results support earlier suggestions that the interdomain sequence is marginally stable under normal cellular conditions (Kretsinger, 1992) and that calcium binding to the carboxyl-terminal domain stabilizes the helical content of the central sequence. Binding of the carboxyl-terminal domain to target proteins appears to function as a conformational switch that is required for binding of the amino-terminal domain. Thus, following target protein association, stabilizing interactions between sites within the carboxyl-terminal domain and the central sequence are disrupted, resulting in the independent rotational dynamics of the amino-terminal domain that is necessary for target protein association and the structural collapse of CaM around the CaM-binding sequence.

Conclusions and future directions

We have demonstrated calcium-dependent structural changes involving the stabilization of a more rigid structure within the interdomain sequence involving Met^{76} to Ser^{81}. To clarify the proposed role of stabilizing interactions between the carboxyl-terminal domain and the central sequence in mediating the high-affinity interaction between CaM and target proteins, future measurements should identify how alterations in the interdomain sequence affects the kinetics of CaM binding to target proteins.

We thank Professors Diana J. Bigelow and Krysztof Kuczera for their insightful comments.

Supported by the National Institutes of Health (grant AG17996) and a postdoctoral fellowship to Z. Q. from the American Heart Association (Kansas Affiliate). The EPR spectrometer was purchased with support from the National Science Foundation (BIR 9214315) and the University of Kansas.

REFERENCES

Altenbach, C., S. L. Flitsch, H. G. Khorana, and W. L. Hubbell. 1989b. Structural studies on transmembrane proteins. II. Spin labeling of bacteriorhodopsin mutants at unique cysteines. *Biochemistry.* 28: 7806–7812.

Altenbach, C., W. Froncisz, J. S. Hyde, and W. L. Hubbell. 1989a. Conformation of spin-labeled melittin at membrane surfaces investi-

gated by pulse saturation recovery and continuous wave power saturation electron paramagnetic resonance. *Biophys. J.* 56:1183–1191.

Altenbach, C., K. Yang, D. L. Farrens, Z. T. Farahbakhsh, H. G. Khorana, and W. L. Hubbell. 1996. Structural features and light-dependent changes in the cytoplasmic interhelical E-F loop region of rhodopsin: a site-directed spin-labeling study. *Biochemistry.* 35:12470–12478.

Babu, Y. S., C. E. Bugg, and W. J. Cook. 1988. Structure of calmodulin refined at 2.2 Å resolution. *J. Mol. Biol.* 204:191–204.

Babu, Y. S., J. S. Sack, T. J. Greenhough, C. E. Bugg, A. R. Means, and W. J. Cook. 1985. Three-dimensional structure of calmodulin. *Nature.* 315:37–40.

Barbato, G., M. Ikura, L. E. Kay, M. Krinks, and A. Bax. 1992. Backbone dynamics of calmodulin studies by ^{15}N relaxation using inverse detected two-dimensional NMR spectroscopy: the central helix is flexible. *Biochemistry.* 31:5269–5278.

Bayley, P. M., and S. R. Martin. 1992. The α-helical content of calmodulin is increased by solution conditions favoring protein crystallization. *Biochim. Biophys. Acta.* 1160:16–21.

Berliner, L. J., J. Grunwald, H. O. Hankovszky, and K. Hideg. 1982. A novel reversible thiol-specific spin label: papain active site labeling and inhibition. *Anal. Biochem.* 119:450–455.

Chattopdhyaya, R., W. E. Meador, A. R. Means, and F. A. Quiocho. 1992. Calmodulin structure refined at 1.7 Å resolution. *J. Mol. Biol.* 228: 1177–1192.

Columbus, L., T. Kálai, J. Jekö, K. Hideg, and W. L. Hubbell. 2001. Molecular motion of spin labeled side chains in α-helices: analysis by variation of side chain structure. *Biochemistry.* 40:3828–3846.

Craig, T. A., D. M. Watterson, F. G. Prendergast, J. Haiech, and D. M. Roberts. 1987. Site-specific mutagenesis of the alpha-helices of calmodulin: effects of altering a charge cluster in the helix that links the two halves of calmodulin. *J. Biol. Chem.* 262:3278–3284.

Crivici, A., and M. Ikura. 1995. Molecular and structural basis of target recognition by calmodulin. *Annu. Rev. Biophys. Biomol. Struct.* 24: 85–116.

Evans, J. N. S. 1995. Biomolecular NMR Spectroscopy. Oxford University Press, Oxford, UK.

Finn, B. E., J. Evanas, T. Drakenberg, J. P. Waltho, E. Thulin, and S. Forsen. 1995. Calcium-induced structural changes and domain autonomy in calmodulin. *Nat. Struct. Biol.* 2:777–783.

Fischer, R., M. Koller, M. Flura, S. mathews, M. A. Strehler-Page, J. Krebs, J. T. Peniston, E. Carafoli, and E. E. Strehler. 1988. Multiple divergent mRNAs code for a single human calmodulin. *J. Biol. Chem.* 263:17055–17062.

Friedberg, F. 1996. Species comparison of calmodulin sequences. *Protein Seq. Data Anal.* 3:335–337.

Gao, J., D. H. Yin, Y. Yao, H. Sun, Z. Qin, Ch. Schöneich, T. D. Williams, and T. C. Squier. 1998. Loss of conformational stability in calmodulin upon methionine oxidation. *Biophys. J.* 74:1115–1134.

Heidorn, D. B., and J. Trewhella. 1988. Comparison of the crystal and solution structures of calmodulin and troponin C. *Biochemistry.* 27: 909–915.

Hühmer, A. F. R., N. C. Gerber, P. R. Ortiz de Montellano, and C. Schöneich. 1996. Peroxynitrite reduction of calmodulin stimulation of neuronal nitric oxide synthase. *Chem. Res. Toxicol.* 9:484–491.

Ikura, M., G. M. Clore, A. M. Gronenborn, G. Zhu, C. B. Klee, and A. Bax. 1992. Solution structure of calmodulin-target peptide complex by multidimensional NMR. *Science.* 256:632–638.

Ikura, M., S. Spera, G. Barbato, L. E. Kay, M. Krinks, and A. Bax. 1991. Secondary structure and side-chain ^{1}H and ^{13}C resonance assignments of calmodulin in solution by heteronuclear multidimensional NMR spectroscopy. *Biochemistry.* 30:9216–9228.

Jaren, O. R., S. Harmon, A. F. Chen, and M. A. Shea. 2000. Paramecium calmodulin mutants defective in ion channel regulation can bind calcium and undergo calcium-induced conformational switching. *Biochemistry.* 39:6881–6890.

Kataoka, M., J. F. Head, A. Persechini, R. H. Kretsinger, and D. M. Engelman. 1991. Small-angle x-ray scattering studies of calmodulin mutants with deletions in the linker region of the central helix indicate that the linker region retains a predominantly alpha-helical conformation. *Biochemistry.* 30: 1188–1192.

Kawasaki, H., and R. Kretsinger. 1995. Calcium-binding proteins 1: EF-hands. *In* Protein Profile, Vol 2. Academic Press, New York. 333–347.

Kraulis. 1991. MOLSCRIPT: a program to produce both detailed and schematic plots of protein structures. *J. Appl. Crystallogr.* 24:946–950.

Kretsinger, R. H. 1992. The linker of calmodulin: to helix or not to helix. *Cell Calcium.* 13:363–376.

Kuboniwa, H., N. Tjandra, S. Grzesiek, H. Ren, C. B. Klee, and A. Bax. 1995. Solution structure of calcium-free calmodulin. *Nat. Struct. Biol.* 2:768–776.

Langren, R., K. J. Oh, D. Cascio, and W. L. Hubbell. 2000. Crystal structures of spin labeled T4 lysozyme mutants: implications for the interpretation of EPR spectra in terms of structure. *Biochemistry.* 39: 8396–8405.

Lanzetta, P. A., L. J. Alverez, P. S. Reinach, and O. A. Candia. 1979. An improved assay for nanomole amounts of inorganic phosphate. *Anal. Biochem.* 100:95–97.

La Porte, D. C., B. M. Wierman, and D. R. Storm. 1980. Calcium-induced exposure of a hydrophobic surface on calmodulin. *Biochemistry.* 19: 3814–3819.

Lee, S. Y., and R. E. Klevit. 2000. The whole is not the simple sum of its parts in calmodulin from *S. cerevisiae*. *Biochemistry.* 39:4225–4230.

Luo, P., and R. L. Baldwin. 1997. Mechanism of helix induction by trifluoroethanol: a framework for extrapolating the helix-forming properties of peptides from trifluoroethanol/water mixtures back to water. *Biochemistry.* 36:8413–8421.

Mchaourab, H. S., M. A. Lietzow, K. Hideg, and W. L. Hubbell. 1996. Motion of spin-labeled side chains in T4 lysozyme: correlation with protein structure and dynamics. *Biochemistry.* 35:7692–7704.

Meador, W. E., A. R. Means, and F. A. Quiocho. 1992. Target enzyme recognition by calmodulin: 2.4 A structure of a calmodulin-peptide complex. *Science.* 257:1251–1255.

Meador, W. E., A. R. Means, and F. A. Quiocho. 1993. Modulation of calmodulin plasticity in molecular recognition on the basis of x-ray structure. *Science.* 262:1718–1721.

Mukherjea, P., J. F. Maune, and K. Bechingham. 1996. Interlobe communication in multiple calcium-binding site mutants of *Drosophila* calmodulin. *Protein Sci.* 5:468–477.

Newton, D. L., M. D. Oldewurtel, M. H. Krinks, J. Shiloach, and C. B. Klee. 1984. Agonist and antagonist properties of calmodulin fragments. *J. Biol. Chem.* 259:4419–4426.

Niggli, V., J. T. Penniston, and E. Carafoli. 1979. Purification of the $(Ca^{2+}$-$Mg^{2+})$-ATPase from human erythrocyte membranes using a calmodulin affinity column. *J. Biol. Chem.* 254:9955–9958.

Pedigo, S., and M. A. Shea. 1995a. Quantitative endoproteinase GluC footprinting of cooperative Ca^{2+} binding to calmodulin: proteolytic susceptibility of E31 and E87 indicates interdomain interactions. *Biochemistry.* 34:1179–1196.

Pedigo, S., and M. A. Shea. 1995b. Discontinuous equilibrium titrations of cooperative calcium binding to calmodulin monitored by 1-D ^{1}H-nuclear magnetic resonance spectroscopy. *Biochemistry.* 34:10676–10689.

Persechini, A., H. W. Jarrett, D. Kosk-Kosicka, M. H. Krinks, and H. G. Lee. 1993. Activation of enzymes by calmodulins containing intramolecular cross-links. *Biochim. Biophhys. Acta.* 1163:309–314.

Persechini, A., and R. H. Kretsinger. 1988. The central helix of calmodulin functions as a flexible tether. *J. Biol. Chem.* 263:12175–12178.

Persechini, A., K. McMillan, and P. Leakey. 1994. Activation of myosin light chain kinase and nitric oxide synthase activities by calmodulin fragments. *J. Biol. Chem.* 269:16148–16154.

Putkey, J. A., K. F. Ts'ui, T. Tanaka, L. Lagrace, J. P. Stein, E. C. Lai, and A. R. Means. 1983. Chicken calmodulin genes: a species comparison of cDNA sequences and isolation of a genomic clone. *J. Biol. Chem.* 258:11864–11870.

Sacks, D. B., M. M. Lopez, Z. Li, and D. Kosk-Kosicka. 1996. Analysis of phosphorylation and mutation of tyrosine residues of calmodulin on its activation of the erythrocyte Ca^{2+}-transporting ATPase. *Eur. J. Biochem.* 239:98–104.

Shea, M. A., B. R. Sorensen, S. Pedigo, and A. S. Verhoeven. 2000. Proteolytic footprinting titrations for estimating ligand-binding constants and detecting pathways of conformational switching of calmodulin. *Methods Enzymol.* 323:254–301.

Shea, M. A., A. S. Verhoeven, and S. Pedigo. 1996. Calcium-induced interactions of calmodulin domains revealed by quantitative thrombin footprinting of Arg37 and Arg106. *Biochemistry.* 35:2943–2957.

Small, E. W., and S. R. Anderson. 1988. Fluorescence anisotropy decay demonstrates calcium-dependent shape changes in photocross-linked calmodulin. *Biochemistry.* 27:419–428.

Sorensen, B. R., and M. A. Shea. 1996. Calcium binding decreases the Stokes radius of calmodulin and mutants R74A, R90A, and R90G. *Biophys. J.* 71:3407–3420.

Sorensen, B. R., and M. A. Shea. 1998. Interactions between domains of apo calmodulin alter calcium binding and stability. *Biochemistry.* 37: 4244–4253.

Strasburg, G. M., M. Hogan, W. Birmachu, D. D. Thomas, and C. F. Louis. 1988. Site-specific derivatives of wheat germ calmodulin. *J. Biol. Chem.* 263:542–548.

Studier, F. W., and B. A. Moffatt. 1986. Use of bacteriophage T7 RNA polymerase to direct selective high-level expression of cloned genes. *J. Mol. Biol.* 189:113–130.

Sun, H., and T. C. Squier. 2000. Ordered and cooperative binding of opposing globular domains of calmodulin to the plasma membrane Ca-ATPase. *J. Biol. Chem.* 275:1731–1738.

Sun, H., D. Yin, L. A. Coffeen, M. A. Shea, and T. C. Squier. 2001. Mutation of Tyr^{138} disrupts the structural coupling between the opposing domains in vertebrate calmodulin. *Biochemistry.* 40:9605–9617.

Sun, H., D. Yin, and T. C. Squier. 1999. Calcium-dependent structural coupling between opposing globular domains of calmodulin involves the central helix. *Biochemistry.* 38:12266–12279.

Tjandra, N., A. Bax, A. Crivici, and M. Ikura. 1999. Calmodulin structure and target interaction *In* Calcium as a Cellular Regulator. E. Carafoli and C. Klee, editors. Oxford University Press, New York. 152–170.

Tjandra, N., H. Kuboniwa, H. Ren, A. Bax. 1995. Rotational dynamics of calcium-free calmodulin studied by ^{15}N-NMR relaxation measurements. *Eur. J. Biochem.* 230:1014–1024.

Török, K., A. N. Lane, S. R. Martin, J.-M. Janot, and P. M. Bayley. 1992. Effects of calcium binding on the internal dynamic properties of bovine brain calmodulin, studied by NMR and optical spectroscopy. *Biochemistry.* 31:3452–3462.

Tsalkova, T. N., and P. L. Privalov. 1985. Thermodynamic study of domain organization in troponin C and calmodulin. *J. Mol. Biol.* 181: 533–544.

Urbauer, J. L., J. H. Short, L. K. Dow, and A. J. Wand. 1995. Structural analysis of a novel interaction by calmodulin: high-affinity binding of a peptide in the absence of calcium. *Biochemistry.* 34:8099–8109.

Venyaminov, S. Y., and J. T. Yang. 1996. Determination of protein secondary structure. *In* Circular Dichroism and the Conformational Analysis of Biomolecules. G. D. Fasman, editor. Plenum Press, New York. 69–107.

Verheyden, P., E. De Wolf, H. Jaspers, and G. Van Binst. 1994. Comparing conformations at low temperature and at high viscosity. *Int. J. Peptide Protein Res.* 44:401–409.

Wriggers, W., E. Mehler, F. Pitici, H. Weinstein, and K. S. Schulten. 1998. Structure and dynamics of calmodulin in solution. *Biophys. J.* 74: 1622–1639.

Wylie, D. C., and T. C. Vanaman. 1988. Structure and evolution of the calmodulin family of calcium regulatory proteins. *In* Calmodulin. P. Cohen and K. B. Klee, editors. Elsevier, Amsterdam. 1–15

Yao, Y., J. Gao, and T. C. Squier. 1996. Dynamic structure of the calmodulin-binding domain of the plasma membrane Ca-ATPase in native erythrocyte ghost membranes. *Biochemistry.* 35:12015–12028.

Yao, Y., C. Schöneich, and T. C. Squier. 1994. Resolution of structural changes associated with calcium activation of calmodulin using frequency domain fluorescence spectroscopy. *Biochemistry.* 33: 7797–7810.

Yao, Y., and T. C. Squier. 1996. Variable conformation and dynamics of calmodulin complexed with peptides derived from the autoinhibitory domains of target proteins. *Biochemistry.* 35:6815–6827.

Yin, D., K. Kuczera, and T. C. Squier. 2000a. Sensitivity of carboxyl-terminus methionines in calmodulin isoforms to oxidation by H_2O_2 modulates ability to activate the PM-Ca-ATPase. *Chem. Res. Toxicol.* 13:103–110.

Yin, D., H. Sun, D. A. Ferrington, and T. C. Squier. 2000b. Closer proximity between opposing domains of vertebrate calmodulin following deletion of Met^{145}–Lys^{148}. *Biochemistry.* 39:10255–10268.

Zhang, M., T. Tanaka, and M. Ikura. 1995. Calcium-induced conformational transition revealed by the solution structure of apo calmodulin. *Nat. Struct. Biol.* 2:758–767.